Interpretation of Migration of Radionuclides in a Rock Fracture Using a Particle Tracking Method

Chung Kyun Park and Pil-Soo Hahn
Korea Atomic Energy Research Institute

Tjalle T. Vandergraaf and Douglas J. Drew
Whiteshell Laboratories
(Received August 30, 1994)

입자추적법을 사용한 암반균열에서 핵종이동 해석

박정균 · 한필수

한국원자력연구소

티. 반더그라프 · 디. 드류

카나다 원자력공사

(1994. 8. 30 접수)

Abstract

A particle tracking scheme was developed in order to model radionuclide transport through a tortuous flow field in a rock fracture. The particle tracking method may be used effectively in a heterogeneous flow field such as rock fracture. The parallel plate representation of the single fracture fails to recognize the spatial heterogeneity in the fracture aperture and thus seems inadequate in describing fluid movement through a real fracture. The heterogeneous flow field was modeled by a variable aperture channel model after characterizing aperture distribution by a hydraulic test. To support the validation of radionuclide transport models, a radionuclide migration experiment was performed in a natural fracture of granite. ^3H_2O and ^{131}I are used as tracers. Simulated results were in agreement with experimental result and therefore support the validity of the transport model. Residence time distributions display multipeak curves caused by the fast arrival of solutes traveling along preferential fracture channels and by the much slower arrival of solutes following tortous routes through the fracture. Results from the modelling of the transport of nonsorbing tracer through the fracture show that diffusion into the interconnected pore space in the rock mass has a significant effect on retardation.

요 약

지하처분된 방사성핵종의 이동 해석방식으로서 입자추적법을 도입하였다. 입자추적법은 암반균열대와 같은 흐름장이 불균일하고 복잡할 때 물질이동을 모사할 수 있는 방법이다. 암반층에서 방사성핵종은 주로 암반사이에 발달한 균열을 따라 이동하는데, 초기연구자들은 균열틈을 평행판 사이의 간격으로 가정하였으나, 실제 균열은 이보다 복잡다양해서 실제 물질 이동과는 상당한 오차가 존재하였다. 이 논문

에서는 이를 극복하기 위해 가변균열폭 국부통로모형을 도입하여, 균열대 내부는 2차원적인 균열폭의 분포를 가지며, 핵종은 균열내에서 상대적으로 큰 균열폭을 따라 이동이 주로 일어나는 국부이동이라는 점을 제시하였다. 또한 개발한 이동모델의 타당성 입증차원에서 자연균열을 가진 화강암을 사용하여 방사성핵종 이동 실험을 수행하였다. 추적자로서 지하수와 같은 이동특성을 가진 삼중수소와 요오드를 사용하였다. 화강암 균열대 특성을 파악하기 위해 균열이 있는 윗 암석면에 11개의 시추공을 뚫고 수리전도시험을 수행하였다. 실험자료와 전산모사치를 비교해 본 결과, 가변균열폭국부통로 개념에 물질이동모델로 입자추적법을 결합한 모델이 암반균열에서 핵종이동 해석방법으로 유용하였다. 또한 핵종은 균열내에서 상대적으로 큰 국부통로를 따라 주로 이동하며, 이동방향과 직각인 암반매질내로 확산도 상당한 비율로 일어났다.

1. Introduction

Assessing the safety of disposed radioactive wastes in an underground repository depends appreciably upon understanding of radionuclide transport mode in the geosphere. In hard rocks, such as granite, most water flow through a fracture system. In order to predict the transport of dissolved radionuclides through the rock it is necessary to take into account the geometry of the fracture system. Flow and transport in a single rock fracture have been considered previously in some of in situ [1, 2] and laboratory experiments. [3, 4, 5] There is considerable evidence from these experiments that water flow in fractured rock is very unevenly distributed, and that most of the water flow occurs over a small proportion of the fracture surface. This phenomenon has been called "channeling". Despite complexities of real fractures, it is necessary to demonstrate that an adequate description can be made of their flow and transport properties. The processes to be considered are advection and dispersion in the fracture plane, coupled with diffusion of the tracer into the stagnant porosity in the rock matrix. This last process is termed "rock matrix diffusion", and has been demonstrated to be a significant process for retarding the migration of radionuclides.

Numerical modelling of groundwater flow in the fractured rock commonly make the assumption that each fracture is idealized as a pair of parallel plates separated by a constant distance which represents the aperture of the fracture. [6, 7, 8] The parallel plate model fails to recognize the spatial heterogeneity in the fracture aperture. The field experiments of solute migration in a single fracture in the Stripa mine showed that the flow was very unevenly distributed along the fracture plane investigated and large areas did not carry any water. [1] The flow paths, or channels, made up only 5−20% of the fracture area. In the parallel plate approach the single fracture in described completely by only the constant fracture. However, the experimental results discussed above indicate that it is impossible to define an equivalent parallel plate aperture consistent with the observed flow and transport phenomena. The flow through a rock fracture is clearly unlike that through a slit between smooth parallel plates. Recent theoretical work has taken into account that the aperture in a real rock fracture take on a range of values. The wide range of aperture values in a single fracture give rise to a very heterogeneous two dimensional system that one might expect the fluid flow to concentrate in a few preferred paths of least fluid resistance. Evidence that flow in fractures tends to coalesce in preferred paths has been found in the field. [1, 2] Tsang et al. [9] proposed a variable aperture channel model for transport through fractured media. Channeling characteristics of flow through a two dimensional fracture were analyzed by Moreno et al. [10]

To develop a mathematical model for solute transport in such a heterogeous flow system, two ways may be possible. One approach attempts to describe

the flow system with an advection-dispersion equation and tries to solve this equation with appropriate boundary conditions. The other approach attempts to simulate the flow system more directly by defining numerical structure that represent physical structures of the system and interact by the physical driving forces as determined. The first approach is termed the model-equation method and usally leads to complex partial differential equations which should be solved numerically. The second one is termed direct simulation method. It requires only that an efficient book-keeping structure be established to control the response of the numerical representations so that all constraints are satisfied. Particle tracking is one of the direct simulation method and is used to trace out flow paths by tracking the movement of infinitely small imaginary particles placed in the flow field. Particle tracking is used to help visualize the flow field or to track contaminant paths. This method has the following advantages over the model equation approach.[11] : Firstly, it is alway mass conservative and the response of this scheme is inherently stable for the time step size, dispersion coefficient and velocity. Secondly, no cumulative numerical dispersion-many of the stability and numerical dispersion problems of Eulerian methods arise from the approximations made to the advective term. The main reason for eliminating the numerical dispersion is the Lagrangian approach to advection computation. This property is the primary motivating factor for the use of the particle tracking method. The only numerical dispersion occurs when average concentration is computed for each grid cell. However, this numerical dispersion is not carried forward in time since particle positions and associated masses are not affected by this averaging process. Thirdly, the accuracy can be easily controlled by specifying the number of particles to be used in the simulation. In addition to these advantages, some weakpoints of this method have been noted : Firstly, a certain amount of statistical random noise is always present in solutions. As more particles are added or by postprocessing the results

with smoothing or filtering methods, the amplitude of the noise decreases. Secondly, the computing time is increased as more particles are used. Applications of this scheme are quite broad but it is frequently used for environmental simulations. Especially it works effectively in the heterogeneous flow field.[12] Usually velocity fields in the fracture are highly variable, and flow paths are highly contorted. Models based on the advection-dispersion equation are adversely affected by numerical dispersion due to the advective solute flux term and are not suitable in this flow system.

In this work, we are going to develop a model describing the migration of radionuclides in a rock fracture, that is, to develop a variable aperture channel model for characterize the fracture plane and a particle tracking scheme for solute transport. Also we are going to validate the developed model by comparing with the result of migration experiment. We therefore present our investigations of flow in two-dimensions, corresponding to the physical situation of flow in a rock fracture, taking into account the variable apertures in the plane of the fracture. By solving for the flow in two dimensions, we attempt to understand the flow characteristics and to identify the key parameters that control the channeling flow pattern, thus providing a way to interpret the fracture field. The other purpose of this study is to incorporate information obtained during the hydraulic characterization of the fracture in the modelling of the radionuclide transport through the rock fracture.

2. Transport Modeling

2.1. Hydraulic Characterization and Aperture Topology

When the flow in the fracture is assumed as a steady state flow in a confined aquifer, the transmissivity between sets of two boreholes, T, may be calculated using equation (1).[1,13]

$$T = \frac{Q}{2\pi\Delta h} \ln\left[\frac{r_w}{2d}\right]$$

(1)

where Q is the volumetric flow rate in cm^3/sec, Δh is the hydraulic head in cm, r_w is the radius of injection/withdrawal borehole in cm, and $2d$ is the distance between injection and withdrawal boreholes. The data obtained in the hydraulic characterization of the fracture may be used to generate an approximate distribution of the fracture aperture, b, across the block using the standard cubic law equation

$$b = \left[\frac{12 \mu T}{\rho g} \right]^{\frac{1}{3}} \tag{2}$$

where μ is the viscosity of the transport solution in $g/cm.sec$, g is the gravitational acceleration in cm/sec^2, and ρ is the density of the transport solution in g/cm^3.

2.2. Flow Field in the Rock Fracture

The fracture plane may be subdivided into subsquares and aperture widths obtained from the hydraulic characterization could be assigned to each subsquares to apply the variable aperture channel concept. The fluid flow through the fracture was then calculated for a constant injection/withdrawal rate as well as for constant pressure conditions. For a constant laminar flow, the volumetric flow rate through a parallel fracture may be written as :

$$Q = \frac{1}{12 \mu} \frac{b^3 W}{L} \Delta P \tag{3}$$

where ΔP is the pressure drop over a length of L and W and μ is the viscosity in $g/cm.s$. Equation (3) may be applied to each of the subsquares enclosed by the grid lines as shown in Figure 1. When the volumetric flow rate from node i to node j is Q_{ij}, the pressure drop from node i to node j can be written

$$\Delta P = P_i - P_j = \frac{Q_{ij}}{\frac{2 b_i^3 \Delta y}{12 \mu \Delta x}} + \frac{Q_{ij}}{\frac{2 b_j^3 \Delta y}{12 \mu \Delta x}}$$

$$= Q_{ij} \left[6\mu \frac{\Delta x}{\Delta y} \left(\frac{1}{b_i^3} + \frac{1}{b_j^3} \right) \right] \tag{4}$$

where P_i is the pressure at node i in $dynes/cm^2$, and

Δx and Δy are the length of x and y coordinate in a subsquare, respectively. Node i implies an index of the ith subsquare in the fracture surface. Then the volumetric flow rate can be rewritten

$$Q_{ij} = C_{ij} (P_i - P_j) \tag{5}$$

where C_{ij} is the flow conductance between nodes i and j in $cm^2 s/g$.

$$C_{ij} = Q_{ij} \left[6\mu \frac{\Delta x}{\Delta y} \left(\frac{1}{b_i^3} + \frac{1}{b_j^3} \right) \right]^{-1}$$

The mass balance at each node is may be written as :

$$\sum_j Q_{ij} = \sum_j C_{ij} (P_i - P_j) = E_i \tag{6}$$

where E_i is the injection rate or withdrawal rate at node i. j stands for the four facing nodes of surrounding subsquares to node i. Except for the nodes at the boundaries, the pressure at each node is unknown to be solved with an iterative numerical method. The flow between adjacent nodes can be calculated using equation (5). After obtaining flow vectors at all nodes, solute transport can be simulated in this flow field.

2.3. Particle Tracking Method for Radionuclide Transport[14, 15]

A particle, which is representing the mass of a solute contained in a defined volume of fluid, moves through a fracture with two types of motion. One motion is with the mean flow along stream lines and the other is random motion, governed by scaled probability.

At the inlet a certain amount of particles were introduced and distributed at each node between flow channels with a probability proportional to the flow rates. Particles are then convected by discrete steps from node to node until they reach the outlet node at which point the arrival time is recorded. Particle movement is regulated by the following algorithm. [16] (Refer Figure 1)
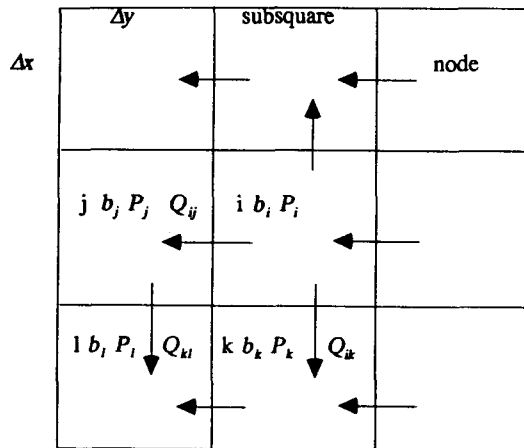
Fig. 1. Schematic Diagram of the Fracture Plane Bounded by Grid Lines

1) At a given node, calculate the volumetric flux across each four faces of the surrounding grid cell as in equation (5). Q_{ij} (j = 1, 2, 3, & 4)

2) Calculate the total outflow from the subsquare.

$$Q_i^t = \sum_{j=1}^{4} Q_{ij}$$

3) Assign a probability to each of the four possible flow directions. Inflow directions receive a probability of zero. Outflow directions receive a probability equal to their fraction of the total outflow from the subsquare.

$$p_{ij} = Q_{ij} / \sum_{j=1}^{4} Q_{ij}$$

4) Generate random number and choose an outflow direction according to the discrete probability distribution.

5) Move particle to the next node in the selected direction at a velocity equal to the total outflow rate from the subsquare. This ensures conservation of total mass flux through the subsquare at any given particle step and, over many passages, conservation of mass flux in each direction.

6) Increment the cummulative travel time by the appropriate amount.

$$t_{cum} = \sum_{i=1}^{n} t_i$$

7) Repeat the above steps until the particle arrives at the withdrawal point.

This procedure is repeated for a specified number of particles to get a stable probability distribution. The residence time for nonsorbing tracers in a given subsquare is determined from the total flow through that subsquare and its volume. The residence time of a particle along each path is obtained as the sum of the residence times in all subsquares through which the particle had passed. Four transport processes are considered in modelling radionuclide transport:

1) advection
2) advection and longitudinal dispersion
3) advection and diffusion into the rock mass
4) advection, longitudinal dispersion and diffusion into the rock mass

3. Experimental

3.1. Preparation of the Rock

A block of granite with dimensions of $81 \times 90 \times 75$cm containing a natural, open fracture, was quarried from a surface exposure. The mineralogical and chemical composition of the granite are listed in Table 1 and 2, respectively. In Table 1, a little amount of secondary minerals can be observed: It means that this rock is a little weathered. Also this rock has an interconnected porosoty of 0.2 to 0.5%. Although this porosity is much lower than in less consolidated rock such as sandstone, the total pore volume is large compared to that of the fracture surface. For a block of granite with dimensions of $81 \times 90 \times 75$cm and a porosity of 0.3%, the total accesible pore volume is 1640cm^3. If the interconnected pore space is not saturated with groundwater prior to performing migration experiments, a small but finite flow of groundwater can be established from the fracture into the unsaturated pore space, giving an enhanced diffusional effect of the groundwater and any con-

Table 1. Mineralogical Composition of the Granite

Mineral	quartz	hematite	zircon	orthoclase	albite	anorthite	magnetite
%	28.5	1.6	0.03	28.3	32.32	4.61	0.84

	apatite	calcite	biotite	sphene
	0.09	0.2	2.94	0.5

Table 2. Chemical Composition of the Granite

Element	SiO2	Al2O2	Fe2O2	FeO	TiO2	MgO	CaO	Na2O	K2O	MnO
%	72.4	14.4	0.79	0.88	0.24	0.47	1.19	3.55	5.03	0.04

taminant away from the fracture. Hence to saturate this rock block, the block was then placed in a neoprene bag, evacuated and backfilled with a groundwater. Following saturation of the block, its outer surfaces were sealed with a silicone rubber material. Stainless steel frames were mounted on both halves of the block and connected to each other by four threaded rods and bolts. Strain gauges were mounted on the four rods and linear variable displacement transducers were attached to the four sides of the block straddling the fracture to detect any movement of one half of the block relative to the other half.

3.2. Preparation of Groundwater

The preparation of groundwater for radionuclide migration experiments has evolved over the years. Ideally, the groundwater should be in geochemical equilibrium with the infilling material in the fractures. The block used in this experiment have been quarried from the surface of granitic rock formations and have most likely been exposed to groundwater from relatively shallow depths or to meteroric water for considerable length of time. To achieve a pseudo-geochemical equilibrium between the groundwater used in this experiment and the fracture infilling materials, a groundwater composition from a particular location is selected. For the experiment, a groundwater with a TDS of 500 mg/l was selected. This groundwater was prepared to the target concen-

tration as given in Table 2. Fifty liter volumes of this groundwater were prepared and contacted with 1 kg of crushed granite for a period of ten months. The final composition of this groundwater is also given in Table 2. This groundwater was used in the migration experiment.

3.3. Hydraulic Test to Obtain Aperture Topology

This technique is normally used in the field, where the fracture cannot be accessed except by intersecting it with boreholes. For the granite block, 11 boreholes was drilled into the block, orthogonally to the fracture and ending at the fracture as shown in Figures 2 and 3. A flow of groundwater through the fracture between pairs of boreholes was initiated using an HPLC pump and the pressure required to maintain the flow was measured with water manometers. The pressure required to maintain a given flow of groundwater through the fracture between the two boreholes is used to calculate the transmissiv ity of the fracture as descrived as equations (1) and (2).

3.4. Radionuclide Migration Test

At the completion of the hydraulic characterization, eight of the mechanical packers were removed from their boreholes and replaced with end-window Geiger-Müller tubes which were sealed into the bor-
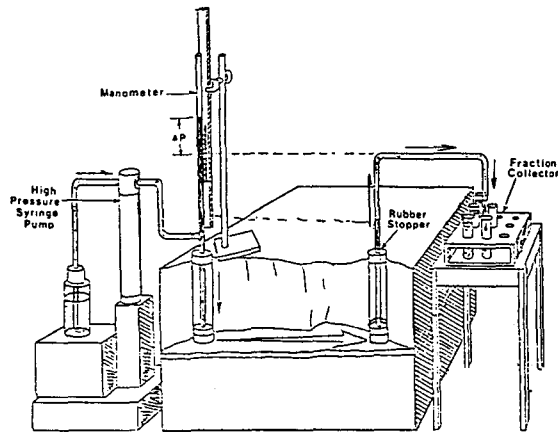
Fig. 2. Schematic Showing the Sample Borehole Orientation and the Experimental Set-up for the Hydraulic Test
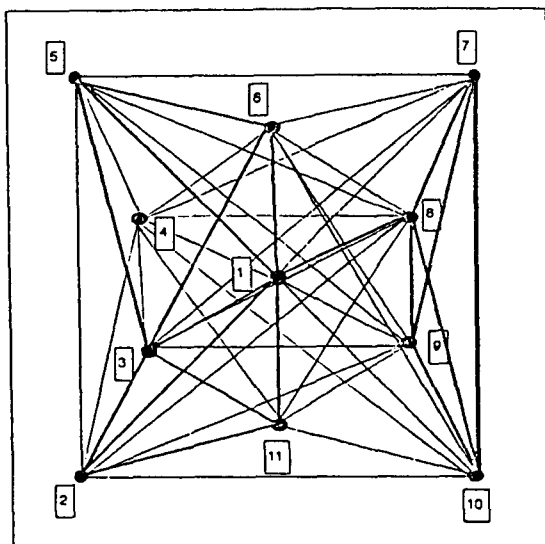

Fig. 3. Arrangement of Boreholes and Graphical Representation of Fracture Aperture Obtained From Borehole-to Borehole Pump Test

eholes in order to measure radioactivity of the flowing radionuclide in the rock fracture. The output of these detectors was routed through a counter/timer board and collected with a data acquisition system .

Ten-mL aliquots of groundwater containing mixtures of ^3H_2O and ^{131}I was injected into borehole BH-7

in separate campaigns and pumped through the fracture at a flow rate of $3 mL/h$ and collected at borehole BH-2 (refer Figure 3). The eluted groundwater was collected using a standard fraction collector. This flow rate is a compromise between two conflicting goals : to maximize the residence time of the tracer in the fracture and to perform the experiments over a reasonable time. At this flow rate, residence time of nonsorbing tracer in the fracture and linear flow velocity of the transport solution are approximately 50 hours and $2 cm/h$, respectively. The eluted groundwater was analyzed for these radionuclides by gamma ray spectrometry and liquid scintillation counter.

4. Results and Discussion

4.1. Aperture Distribution and Flow Field in the Fracture Plane

The calculations of the fracture aperture distributions from the transmissivity values were performed using equation (2). This calculation gives the value along a straight line connecting a set of boreholes. Graphical representation of fracture apertures obtained from borehole-to-borehlole pump tests is shown in Figure 3. The thickness of the line segments between the boreholes is roughly proportional to the average fracture aperture. The fracture surface was divided into a matrix of 16×18 sub-squares. All sub-squares along each line segment connecting a pair of boreholes were assigned a fracture aperture value associated with that line segment. For subsquares containing more than one line segment, a mean value was calculated from the aperture values of thes e line segments. For sub-squares containing no line segment, a mean value was calculated from the aperture values of the surrounding sub-squares. These data points, with their x and y coordinates and aperture value were entered into a graphic program SUR-FER which uses the Kriging technique to characterize aperture topology. Two dimensional distribution in

the fracture surface is shown in Figure 4. It suggests that there are two zones with relatively wide apertures around between borehole BH-7 and BH-10 as well as borehole BH-3, separated by a region with smaller aperture around right region between borehole BH-6 and BH-11. Population density of the aperture value is shown in Figure 5. It shows that relatively low aperture value consists the major portion of the aperture population, while, even though the
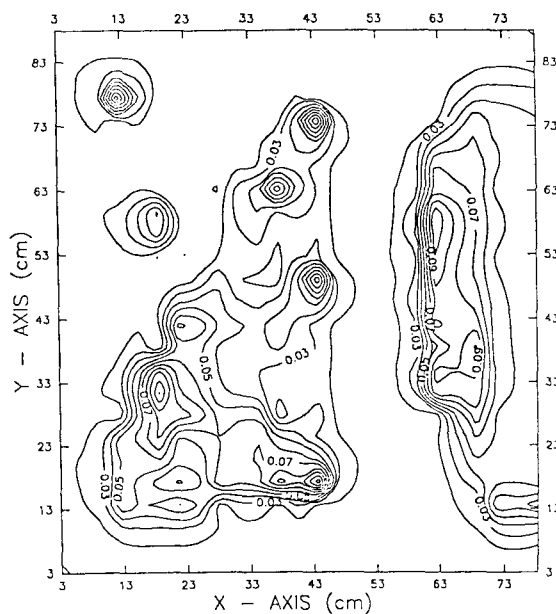

Fig. 4. Topographic Map of Fracture Aperture Distribution
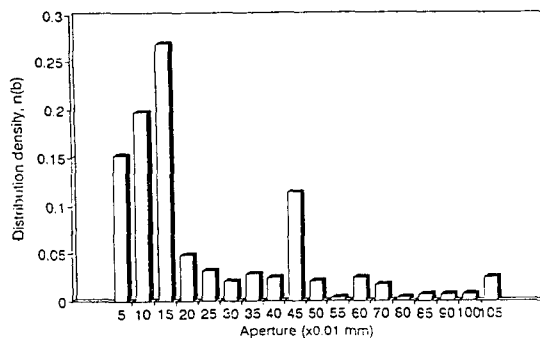
Fig. 5. The Aperture Density Distribution Over the Two-dimensional Fracture.

portion of the large aperture value is of little, the effect on the flow can be dominant. That is, the major portion of flow of groundwater will flow through larger aperture path. The simulated pressure field is shown in Figure 6. The value in Figure 6 is the pressure field is shown in Figure 6. The value in Figure 6 is the pressure in $dynes/cm^2$. The pressure drop between the injection and withdrawal boreholes are about 22 $dynes/cm^2$. Comparing Figure 4 to Figure 6, there are large apertures and small pressure drop around between borehole BH-7 and BH-10 while small apertures and large pressure drop around right region between borehole BH-6 and BH-11which may act as a flowing barrier to flow from borehole BH-7 to BH-2. Recall that the boundary conditions employed to solve the flow through the system are the constant head boundary condition ; that is, injection node is at the higher constant pressure P_1 and the withdrawal node is at lower constant pressure P_2. The flow between adjacent nodes can be calculated using Equation (3). Little flow could be obtained from borehole BH-4, indicating that the fracture was tight at that location.
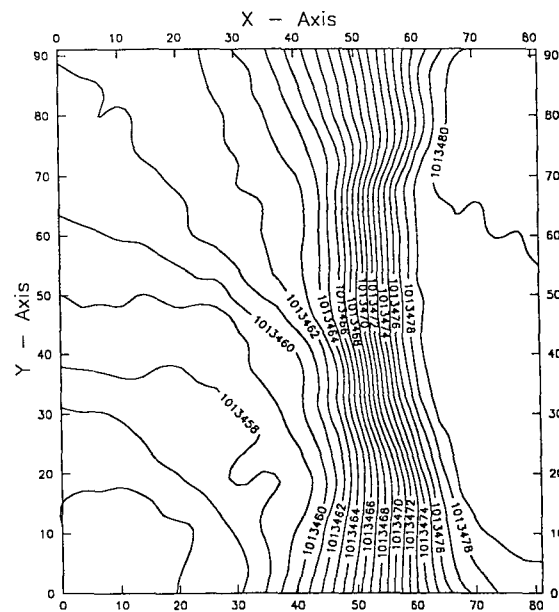

Fig. 6. Topographic Map of Pressure Distribution in the Fracture

4.2. Particle Tracking Process for Solute transport

Preliminary calculations have been carried out for a total number of input particles ranging from 10^2 to 10^6 in order to investigate the effect of the number of particles on the elution curves because the numerical accuracy is considered to dependent on the number of particles used.[15] As expected, the calculation using the larger number of particles gives the better approximation as shown in Figure 7. When 100 particles are used, the elution curve has roughly same residence time but very small variance comparing to other cases, especially it does not show tailing effect. When 1,000 particles are used, the elution curve has roughly same residence time and variance but it shows numerous peaks. When the number of particles becomes 5,000, the elution curve approachs a stable shape as the experimental result. There is no significant improvement in the numerical results when the total number of particles is more than 10^5. This may be resulted from that the random values generated by a computer subroutine are pseudo-random processes rather than the perfect random process. Calculations using more than 5,000 particles are adequate since they yield elution curves that have few spurious artifacts due to the finite number
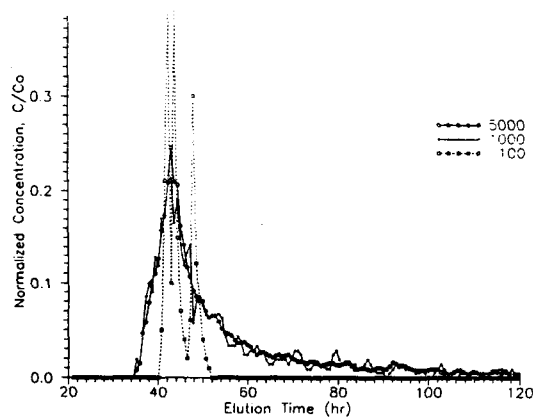

Fig. 7. Comparision of Elution Curves with the Number of Particles

Table 3. Chemical Composition of the Groundwater

Species	Initial Conc. (mg/l)	Final Conc. (mg/l)
Na^+	57.8	57.4
K^+	0.07	1.63
Ca^{2+}	101	74.5
Mg^{2+}	0.025	0.226
Fe	0.0164	⟨ 0.01
Si	⟨ 0.04	1.4
Al	⟨ 0.1	0.179
F^-	⟨ 0.05	⟨ 0.05
Cl^-	182	187
NO_3^-	⟨ 0.16	⟨ 0.16
SO_4^{2-}	⟨ 0.1	0.28
Alk. (as $CaCO_3$)	131	113
pH	8.3	8.0

of particles employed. Thus 10,000 particles are chosen in this study.

4.3. Migration Plume and Channeling Flow

Migration plumes of nonsorbing tracer simulated with the computer program are shown in Figures 8. (a) −8.(d). Those figures show that major migation plume moves from the injection borehole, BH-7, via BH-8 and BH-9, to the withdrawal borehole, BH-2. That is, major flow stream moves through large apertures. From the point of view of flow and transport, a fracture is described by the aperture between the fracture surfaces. Since the fracture surface is rough and undulating the apertures vary spatially. There are areas where the fracture surfaces are in contact and the aperture is zero like the area around BH-4. Fluid flowing through a saturated fracture seeks out the least resistive pathways usually composed of largest apertures. The main flow is therefore expected to occur through a few channels in the fracture plane from BH-7, via BH-8 and BH-9, to BH-2. Areas with small apertures around BH-4 will usually have very little flow because the local resistance to the flow is inversely proportional to the cube of the local aperture. Areas with large apertures do not necessarily
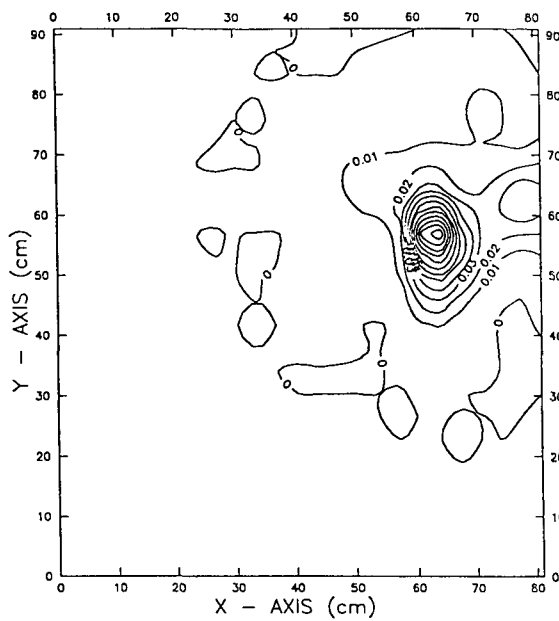
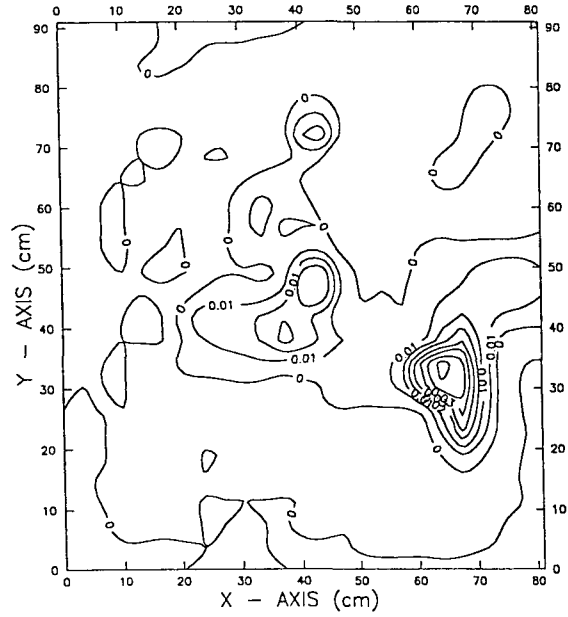**Fig. 8.1.** Contours of Migration Plume at 10 hours in the Fracture

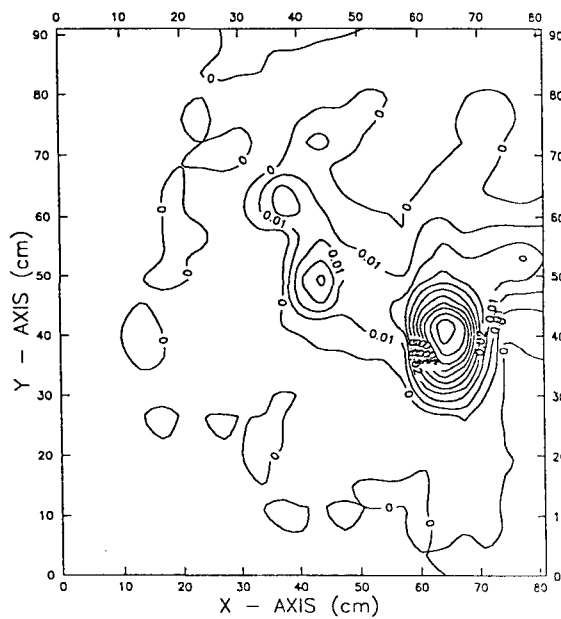**Fig. 8.3.** Contours of Migration Plume at 30 hours in the Fracture

Fig. 8.2. Contours of Migration Plume at 20 hours in the Fracture
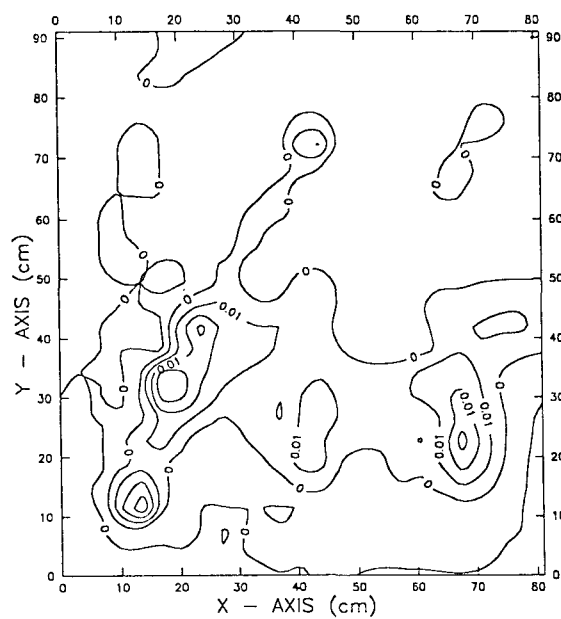

Fig. 8.4. Contours of Migration Plume at 40 hours in the Fracture

have large flow because they may be isolated from the main flows by constrictions around them. Our interest is not only in the average flow and how it differs from that through a pair of parallel plates ; rather, we shall focus our study on cases where channeling of flow dominates. Our goal is to study the channeling character of tracer transport through the fracture and to consider their implications on field mesurements and data analysis. Those simulation results are consistent with the on-line borehole counting of $^{131}I^-$ shown in Figure 9. The responses of the eight end window probes for the ^{131}I plume passing through the fracture are shown in Figure 9. These plots clearly show the different arrival times for the ^{131}I. In addition, these plots confirm the considerable amount of tailing observed in the elution profiles. The response of the eight end-window probes in borehole BH-1 and BH-11 to the successive pulses of ^{131}I, is shown in Figure 8, normalized to the peaks of the response curves. The arrival times for the ^{131}I peaks were much closer to each other in BH-11 than in BH-1, even though BH-1 is closer to the inlet borehole (BH-7). This observation suggests that flow between BH-7 and BH-11 was more rapid than that between BH-7 and BH-1. The differences in the extent of retardation between the boreholes may be due to differences in the mineralogy along the flow paths. The normalized elution profiles for ^3H_2O and ^{131}I are presented in Figure 10. Both curves show multi-peak ; an evidence of channeling flow. Two
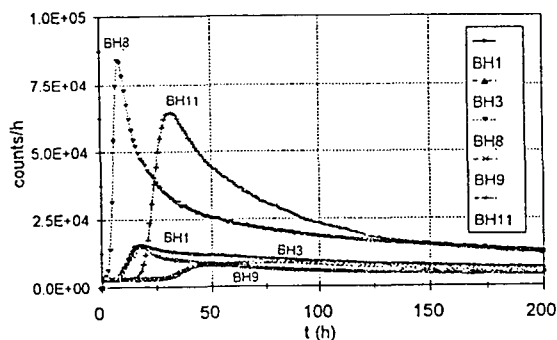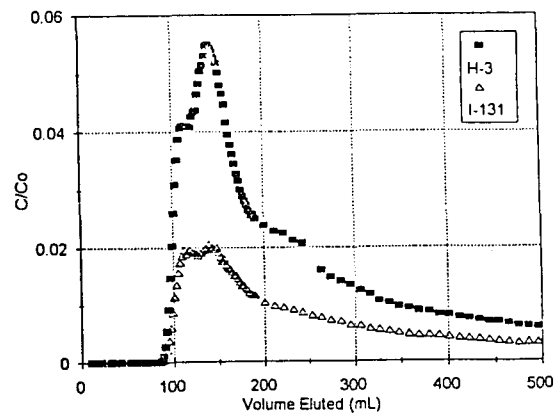

Fig. 10. Normalized Elution Profiles for ^3H_2O / ^{131}I experiment

curves also show same retention time. However, the magnitude of C/Co and cumulative C/Co or recovery show a big difference. The ^{131}I recovery was 56% compared with 93% for ^3H_2O. This suggests that part of the injected ^{131}I was sorbed on the fracture surfaces, either as iodate or assimilated by micro-organisms in the fracture.[3] Iodine can exit as iodide and iodate in this groundwater condition. Iodide hardly sorbs on any minerals while iodate sorbs on minerals such as chlorite and hematite.[17] The presence of microbial activity in the system was confirmed in a purple colored deposit that formed along the length of the Teflon outlet tubing leading from the fracture to the fraction collector and eventually led to partial plugging of this tubing.

4.4. Migration Mechanism

Figure 11 shows the elution curve that was obtained from the residence times of the 10,000 particles. When sorption, hydrodynamic dispersion and diffusion into the rock mass are considered, different particles in the same subsquare will have different residence times. The residence times for these particles can be expressed as a probability density function which in turn can be regarded as the elution concentration of a pulse injection. Integrating this curve over time gives a cumulative elution profile as shown in Figure 12. In general, the cummulative elution curves
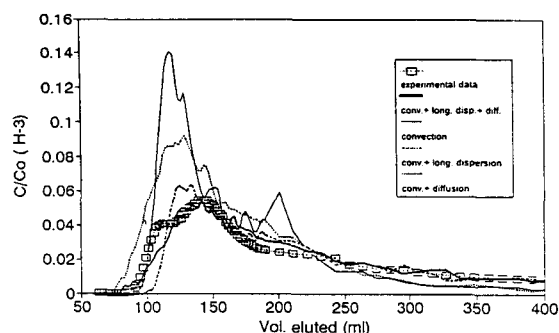

Fig. 9. Response of End-window Probes to Injected ^{131}I Band Input
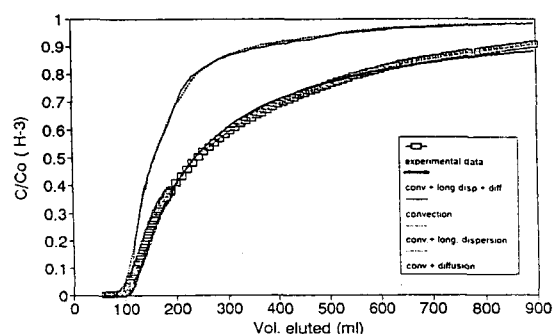
Fig. 11. Calculated and Experimental Elution Curves for ³H₂O

Fig. 12. Calculated and Experimental Cumulative Elution Curves for ³H₂O

[131]I are presented in Figure 10. Both curves show multi-peak ; an evidence of channeling flow. Two curves also show same retention time. However, the magnitude of C/Co and cumulative C/Co or recovof tracer transport in two dimensions through these variable aperture fractures have a fast rise at early times, since the majority of particles take the fastest flow paths ; then there is a long tail in the breakthrough curve due to a small fraction of particles meandering through the fracture with extremely small volumetric flow rates. Figure 12 shows that reasonably good agreement was obtained between experimental and predicted results when diffusion into the rock mass was included. This agreement suggests that, for ³H₂O at least, diffusion into the rock mass has a greater effect on radionuclide transport than hydrodynamic dispersion along the individual flow path or dispersion

due to the channeling. Differences in residence times of the ³H₂O in individual flow channels result in a large overall dispersion. The remaining discrepancies between experimental and calculated results are due to the uncertainties in the fracture aperture distribution.

5. Conclusions

The particle tracking method was applied successfully in a heterogeous flow field such as rock fracture. The hydraulic test to obtain aperture distribution in the fracture was adequately described the variable aperture field. Computer simulation results show that migration of the radionuclides through a rock fracture seeks out the least resistive pathways composed of largest aperture. The end-window Geiger-Müller probes in the boreholes allow the plume of radionuclides through the fracture to be mapped in real time and show the presence of more than one flow path flowing through the more open zones of the fracture. The extent of tailing of ^{131}I, a conservative tracer, was extensive and may have been due to the interaction of ^{131}I as iodate with fracture infilling minerals or to microbial activity in the fracture.

The observed retardation supports flow through relatively open channels in the fracture. Results from the modelling of the transport of nonsorbing tracers through the fracture show that diffusion into the interconnected micropore space in the rock mass has a significant effect on retardation.

Nomenclature

b	fracture aperture in cm
C_{ij}	flow conductance between nodes i and j in $cm^4 s/g$
$2d$	distance between injection and withdrawal boreholes
E_i	injection rate or withdrawal rate at node i in cm^3/s
g	gravitational acceleration in cm/sec^2
h	hydraulic head in cm

μ viscosity of the transport solution in $g/cm. sec$
ρ density of the transport solution in g/cm^3
P_i pressure at node i in $dynes/cm^2$
p_{ij} probability of the flow from node i to node j
Q_{ij} volumetric flow rate from node i to node j in cm^3/s
r_w radius of injection/withdrawal borehole in cm
t_i residence time of a particle in node i
t_{cum} cummulative travel time of a particle along the flow path
T transmissivity in cm^2/sec

References

1. H. Abelin, I. Neretnieks, S. Tunbrant, and L. Moreno, Final report of the migration in a single fracture : Experimental results and evaluation. Stripa Proj. Sren. Karnbransleforsorjning Tech. Rep. 85−03, Nucl. Fuel Safety Proj., Stockholm, Sweden, May (1985).

2. P.A. Hsieh, S.P. Neuman, G.K. Stiles, and E.S. Simpson. Field determination of three-dimensional hydraulic conductivity tensor of anisotropic media, 2, Methodology and application to fractured rock, Water Resour. Res., 21(11), 1667−1676, (1985).

3. T.T. Vandergraaf, C.K. Park, D.J. Drew, Migration of conservative and poorly sorbing tracers in granite fractures, Proceedings of the 5th international high level radioactive waste management conference, ASCE, Las Vegas, May, (1994).

4. A.B. Gureghian, C.J. Noronha and T.T. Vandergraaf, Large Block Migration Experiments INTRAVAL Phase 1, Test Case 9. BMI/OWTD-7, Office of Waste Technology Development, Willowbrook, Illinois, (1990).

5. L. Moreno, I. Neretnieks, and T. Eriksen, Analysis of some laboratory tracer runs in natural fissures, Water Resour. Res., 21(7), 951−958, (1985).

6. Y.M. Lee, W.J. Cho, K.W. Han, and H.H. Park, Verification of a nuclide migration model by comparing with other models, J. of the Kor. Nucl. Soc. 22(3) 304, 1990

7. D.K. Keum, W.J. Cho, P.S. Hahn, and H.H. Park, Study on the radionuclide migration modeling for a single fracture in geologic medium, J. of Kor. Nucl. Soc. 26(3), (1994)

8. C.K. Park, Lee, H.S., Han, K.W., Park, H.H., A preliminary safety analysis for selecting candidate disposal sites 12th Int. Symposium on the scientific basis for nuclear Waste management, Germany, (1988).

9. Y.W. Tsang, C.F. Tsang, I. Neretnieks, and L. Moreno, Flow and tracer transport in fracture media-A variable-aperture channel model and its properties, Water Resour. Res., 24(12), (1988)

10. L. Moreno, Tsang C.F., Hale, F.V. and Neretnieks, I. Flow and tracer transport in a single fracture, Water Res. Res. 24, 2033, (1988).

11. J.F. Washburn, F.E. Kaszeta, C.S. Simmons, and C.R. Cole, Multicomponent mass transport model, PNL-3179, (1980)

12. M.P. Anderson and W.W. Woessner, Applied groundwater modeling, chap. 11, Academic Press, (1992)

13. J. Bear, Hydraulics of Groundwater, McGraw-Hill, (1979).

14. R. Yamashita and H. Kimura, Particle-tracking technique for nuclide decay chain transport in fractured porous media, J. of Nuclear Sci. and Tech. 27, 1041, (1990).

15. L. Moreno and I. Neretnieks, Flow and nuclide transport in fractured media, J. of Contaminant Hydrology, 13, pp. 49−71, (1993).

16. A.J. Desbarats, Macrodispersion in Sand-Shale Sequences, Water Resour. Res., 26(1), 153, (1990).

17. K.V. Ticknor and Y. -H. Cho, The interaction of iodide and iodate with granitic fracture-filling minerals, J. of Radional. Nucl. Chem. 140, 75, (1990).